tvst

Article

Changes After a Month Following Micropulse Cyclophotocoagulation in Normal Porcine Eyes

So Min Ahn[1], Mihyun Choi[1], Seong-Woo Kim[1], and Yong Yeon Kim[1]

[1] Department of Ophthalmology, Korea University College of Medicine, Seoul, Korea

Correspondence: Yong Yeon Kim, Department of Ophthalmology, Korea University Guro Hospital 148, Gurodong-ro, Guro-gu, Seoul 08373, South Korea. e-mail: yongykim@korea.ac.kr
Seong-Woo Kim, Department of Ophthalmology, Korea University Guro Hospital 148, Gurodong-ro, Guro-gu, Seoul 08373, South Korea. e-mail: ksw64723@korea.ac.kr

Received: August 13, 2021
Accepted: October 11, 2021
Published: November 9, 2021

Keywords: micropulse; transscleral cyclophotocoagulation; uvea; ciliary muscle; pars plicata; retina

Citation: Ahn SM, Choi M, Kim SW, Kim YY. Changes after a month following micropulse cyclophotocoagulation in normal porcine eyes. Transl Vis Sci Technol. 2021;10(13):11, https://doi.org/10.1167/tvst.10.13.11

Purpose: To analyze the effects on the uvea, including the pars plicata and ciliary muscle, and retina in normal porcine eyes after performing micropulse transsIceral cyclophotocoagulation (MP-TSCPC) with the different energy levels, and conventional continuous wave transsIceral cyclophotocoagulation.

Methods: MP-TSCPC was performed in a total of 15 eyes at the different energy levels of 60 J, 120 J, 180 J, 240 J, and 300 J, respectively. Continuous wave transsIceral cyclophotocoagulation was performed in three eyes and the other three eyes were controls. The eyes were enucleated after a month following the laser treatment and the uvea and retina were analyzed using hematoxylin and eosin staining and immunohistochemistry staining.

Results: After MP-TSCPC 60 J, the expression of α-smooth muscle actin (α-SMA) and glial fibrillary acidic protein in the ciliary muscle was increased, although there was no structural change in pars plicata. After MP-TSCPC 120 J, partial destruction of the ciliary epithelium was observed in pars plicata, and the retinal thickness was increased. After MP-TSCPC 240 J and 300 J, the structural destruction of the pars plicata and ciliary muscle was observed, and the expression of α-SMA and glial fibrillary acidic protein in pars plicata and the expression of α-SMA in ciliary muscle were increased.

Conclusions: Histologic changes in the uvea and peripheral retina were different based on the energy levels of MP-TSCPC. In particular, MP-TSCPC with low energy levels mainly affected the ciliary muscle, while MP-TSCPC with high energy levels affected both the ciliary muscle and pars plicata. Our results may imply a possibility of intraocular damage with MP-TSCPC in humans.

Translational Relevance: Based on our research, it is possible to infer the possibility of intraocular damage in humans according to the different levels of energy in the clinic.

Introduction

There are various ophthalmology treatment options to manage glaucoma including medications, lasers, and surgical procedures. In traditional laser treatment, photocoagulation is one of the mechanisms underlying the therapeutic effects that has been effectively induced through thermal interaction.[1] Continuous wave transscleral cyclophotocoagulation (CW-TSCPC) using a diode laser is one of conventional laser treatment used in refractory glaucoma by photocoagulation mechanism.[2–5] CW-TSCPC directly destroys the ciliary epithelium, causing reduced production of aqueous humor in the eye, and thereby lowering the intraocular pressure (IOP).[2,3]

Recently, micropulse laser treatment has been used as an alternative to conventional continuous wave lasers.[1] Micropulse transscleral cyclophotocoagulation (MP-TSCPC), a type of micropulse laser treatment, has similar clinical effectiveness to CW-TSCPC in patients with glaucoma.[3,6] Unlike CW-TSCPC, wherein energy is emitted in a continuous wave mode, MP-TSCPC uses a micropulse mode, emitting less energy because of an on–off cycle. Ocular complications after MP-TSCPC are fewer because it does not cause direct destruction of the ciliary epithelium; meanwhile, CW-TSCPC can cause serious visual

loss and challenges, including hypotony and phthisis bulbi, owing to the direct destruction of the ciliary body.[3] Therefore, the risk of complications in MP-TSCPC is lowered by decreasing other tissue damage.[3–5] However, the mechanism of MP-TSCPC and the degree of histologic damage resulting from the energy changes are unclear. It is implied that the thermal energy of MP-TSCPC affects the ciliary muscle, a part of the uvea.[3]

Because of the location of the laser application, both CW-TSCPC and MP-TSCPC can affect the pars plicata or ciliary muscle, which is a part of the uvea. They may further affect the retina adjacent to the choroid, which is also a part of the uvea.[7] Because conventional CW-TSCPC generates complications in the choroid and retina after laser treatment, such as uveitis, choroidal detachment, and retinal detachment, MP-TSCPC is expected to affect the uvea and retina.[8,9]

Therefore, in this study, we investigated the effects and histologic changes of the uvea, including the pars plicata and ciliary muscle, and retina of porcine eyes after MP-TSCPC at different energies. Furthermore, we confirmed the advantages of MP-TSCPC over the conventional CW-TSCPC by comparing the differences in their effects.

Methods

Animals

Of 21 female normal micropigs, the right eyes of 18 were treated using laser treatment, and the right eyes of the remaining three micropigs were used as controls. The mean body weight of the micropigs was 25.97 kg (range, 22.7–29.4 kg), and their mean axial length, measured using A-scan ultrasound examination, was 20.36 ± 0.64 mm.

Before laser treatment, all the micropigs were premedicated and anesthetized. Premedication was performed by subcutaneous injection of atropine (0.05 mg/kg, Je-Il atropine sulfate; Je-Il Pharmacy, Daegu, South Korea) and intramuscular administration of azaperone (4 mg/kg, SF Azaperone; SF Corp., Ansan, South Korea) and xylazine (1 mg/kg, Rompun; Bayer Corp., Pittsburgh, PA). Anesthetic induction was performed by intravenous administration of alfaxalone (1 mg/kg, Alfaxan; Vetoquinol, Lure, France) through the marginal auricular vein. After intubation, the pigs were maintained under general anesthesia with inhalation of 1.5% to 2.0% isoflurane gas (Ifran; Hana Pharm Co., Ltd., Gyeonggi-do, South Korea). The anesthesia ventilator was set at a tidal volume of 8 to 12 mL/kg, frequency of 10 to 20/min, maximum pressure of 20 to 25 cm H_2O, and an inspiratory oxygen fraction of approximately 30% during the experiment.

Under general anesthesia in the dorsoventral position, the IOP was measured using a portable tonometer (iCare; iCare ic200, Innokas Medical Oy, Finland) before and 30 minutes after laser intervention. The IOP was also measured under anesthesia, 4 weeks after laser treatment. All IOP measurements were checked repeatedly (six times).

All experimental procedures in this study were conducted in accordance with the Association for Research in Vision and Ophthalmology (ARVO) Statement for the Use of Animals in Ophthalmic and Vision Research (ARVO Animal Policy). The study was approved by the Institutional Animal Care and Use Committee of the Korea University College of Medicine in Seoul, South Korea.

Intervention With Transscleral Cyclophotocoagulation Laser

TSCPC was performed using a laser machine (MicroPulse; IRIDEX, CYCLO G6 Glaucoma Laser System, Mountain View, CA) capable of performing both MP-TSCPC and CW-TSCPC laser treatments using a semiconductor diode laser with an 810-nm infrared wavelength.[6]

An eyelid speculum was inserted into the right eye of the pig under general anesthesia, and hydroxypropyl methylcellulose (Hycell solution 2%, Samil, South Korea) was applied to the surface of the cornea and conjunctiva to lubricate and to facilitate the motion of the laser probe over the bulbar conjunctiva.

MP-TSCPC emitted energy with a power of 1800 mW and a duty cycle of 31.3%, which translated to 0.5 ms of on-time and 1.1 ms of off-time and was performed with a laser probe (Mp3 probe; Iris Medical Instruments, Mountain View, CA).[3,10,11] The total laser energy at different levels 60 J, 120 J, 180 J, 240 J, and 300 J were delivered according to the change in duration time 107 seconds, 213 seconds, 320 seconds, 426 seconds, and 532 seconds, respectively. Based on previous reports, the laser probe was applied to the scleral area, 1 mm away from the corneal limbus, in a continuous sliding arc motion (sweeping motion), in the directions of clock positions 9:30 to 2:30 and 3:30 to 8:30, excluding the 3 and 9 o'clock positions.[4,6,11,12] The continuous sliding arc motion was slowly performed for approximately 10 seconds in each hemisphere.

The CW-TSCPC laser emitted energy in the continuous wave mode with a power of 1500 to 1700 mW and a duration of 2.5 seconds with the application of a laser probe (G-probe; Iris Medical Instruments) to the edge of the corneal limbus. It was performed in 10 locations of the superior and inferior sclera, except at the 3 and 9 o'clock positions, and a total 80 J laser energy level, known as the clinically safe range of laser intensity for irradiation.[2,5]

In this experiment, CW-TSCPC and each of the total energy levels of 60 J, 120 J, 180 J, 240 J, and 300 J in MP-TSCPC were applied to the right eyes of three micropigs.

Histologic Examination and Immunohistochemistry

Euthanasia was performed by intravenous injection of KCl (2 mM/kg) 4 weeks after laser treatment for 21 porcine eyes, including 18 eyes that underwent TSCPC, and 3 normal control eyes. After euthanasia, enucleation was performed. The enucleated eyes were immersion-fixed in Davidson's solution for 24 hours, dehydrated, and paraffinized. The tissues, including the areas of the pars plicata and the ciliary muscle, were sectioned at a thickness of 4 µm per eye in four locations, 1, 5, 7, and 11 o'clock positions, and further stained with hematoxylin and eosin (H&E). The tissues of the retina at the peripheral area were also sectioned at a thickness of 4 µm in three locations per eye and further stained with H&E. The slides were examined using a light microscope (BX-53; Olympus Corp., Tokyo, Japan) to analyze the pathological changes in the pars plicata, ciliary muscle, and retina and photographed with a digital camera (INFINITY3-1UR; Lumenera Corp., Ottawa, ON, Canada), as previously described.[13,14]

The tissue sections were deparaffinized, rehydrated, and treated with microwave heat in antigen retrieval buffer (1 mM EDTA, 0.05% Tween 20, pH 8.0). After washing with phosphate-buffered saline (PBS), the sections were blocked with 4% horse serum, followed by primary antibody incubation overnight at 4°C. To stain glial fibrillary acidic protein (GFAP), the sections were incubated with anti-GFAP (Novus Biological, Littleton, CO) for 2 h at 25°C and incubated with Alexa Fluor 594-conjugated goat anti-mouse secondary antibody for 1 h. Immunohistochemical staining for α-smooth muscle actin (α-SMA) (Novus Biological) and cyclo-oxygenase-2 (COX-2) antibody (LSBio, LifeSpan BioSciences, Inc., Seattle, WA) was performed according to the manufacturer's protocols. Nuclei were stained with 4,6-diamidino-2-phenylindole (DAPI) (AnaSpec Inc., Fremont, CA). Stained cells were observed using fluorescence microscopy (T2000-U; Nikon, Tokyo, Japan).[14]

Image Analysis and Statistical Analysis

The histologic changes of the pars plicata, ciliary muscle, and retina in the H&E-stained tissues were compared and analyzed for the porcine eyes subjected to MP-TSCPC or CW-TSCPC and the control eyes. Pars plicata is defined as the area that includes ciliary processes with nonpigmented and pigmented ciliary epithelia, and ciliary stroma of the ciliary body. The ciliary muscle is defined as the area composing various ciliary muscle fibers of the ciliary body and is located between the area of the pars plicata and sclera. Trabecular meshwork (TM) length and retinal thickness were measured in the control and eyes after laser intervention, respectively, using ImageJ software (version 1.51; National Institutes of Health, Bethesda, MD) to determine whether there were any effects in these parameters after laser intervention compared to the control and also compared to different energy levels of laser applications. The TM length is defined from the tip of the scleral spur to the end of Schwalbe's line (Fig. 1).[15,16] The retinal thickness is defined from the ganglion cell layer to the photoreceptor layer. The TM length was measured in four locations per eye, and the retinal thickness was measured at three locations for each tissue section, with a total of nine locations for each eye.

Additionally, the retina was stained with GFAP to confirm the glial proliferation. GFAP staining and α-SMA staining for myofibroblast expression were performed in the area of the pars plicata and the area of the ciliary muscle to examine the inflammation of the uvea. COX-2 protein staining was performed on the pars plicata to analyze the expression of the ciliary epithelial cells and inflammation. The area expressing immunohistochemical staining was automatically measured for each section using ImageJ software.

Statistical analyses were conducted using a Mann–Whitney U test to compare the two groups, and the Kruskal–Wallis test was used to compare several groups. Wilcoxon signed rank test was used to compare difference in IOP baseline and 4 weeks after laser treatment. Friedman test was used to compare difference in IOP baseline, 30 minutes after laser treatment and 4 weeks after laser treatment. Data are presented as means ± standard deviations, and differences were considered statistically significant at a P value of less than 0.05.

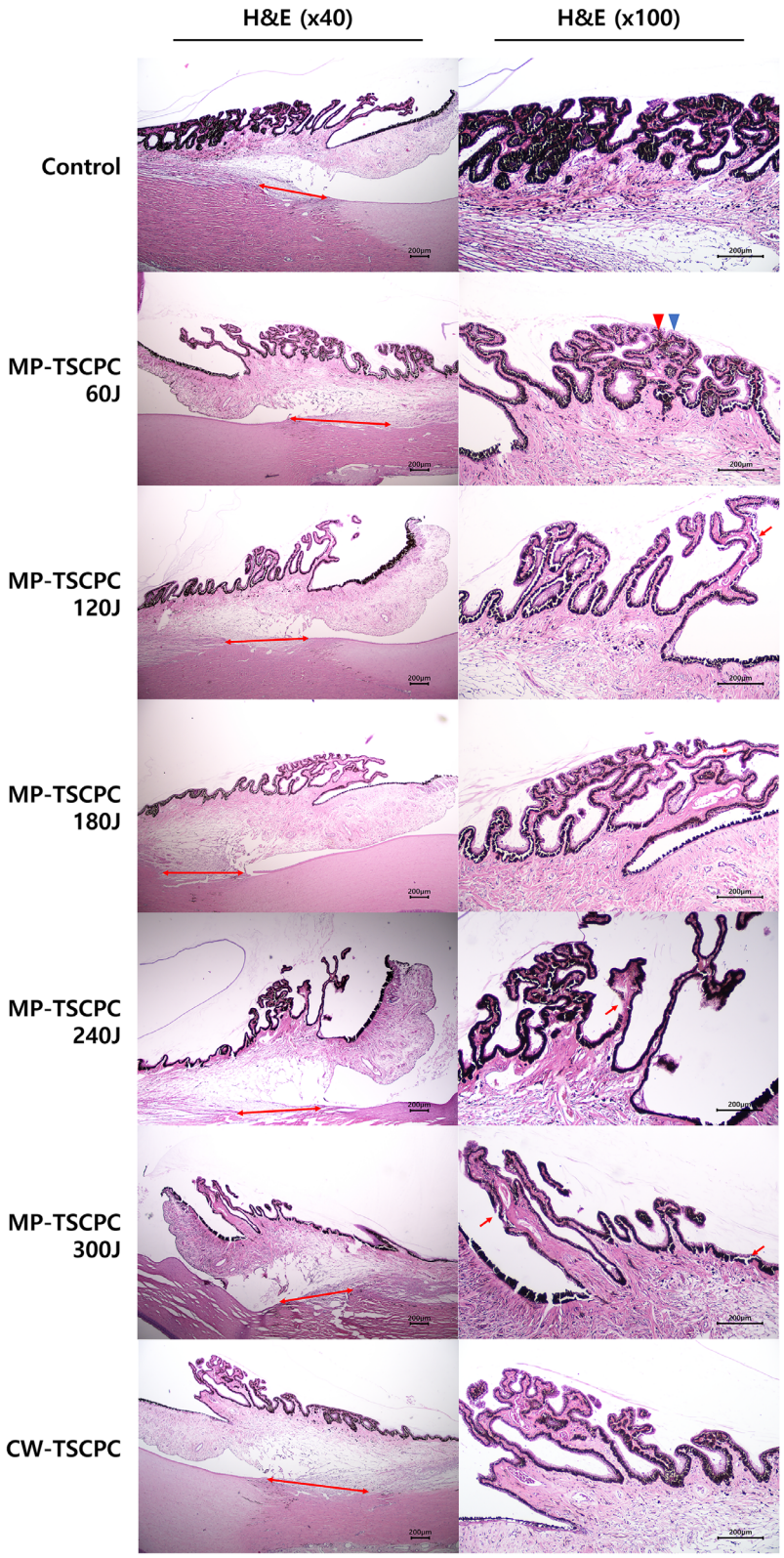

Figure 1. Histologic examination of the pars plicata using H&E staining in control and after MP-TSCPC 60 J, 120 J, 180 J, 240 J, and 300 J, and CW-TSCPC. The TM lengths (*red double arrow* in the left column) in the MP-TSCPC 60 J, 120 J, 180 J, 240 J, and 300 J, and CW-TSCPC groups have increased compared with the control group. The nonpigmented ciliary epithelium layer (*blue arrowhead* in right column) and pigmented ciliary epithelium layer (*red arrowhead* in right column) in the pars plicata are intact following MP-TSCPC 60 J. Partial disruption of the nonpigmented and pigmented ciliary epithelium layers in the pars plicata is observed (*red arrow* in the right column) following MP-TSCPC 120 J, 240 J, and 300 J. The stromal destruction in the pars plicata was observed (*red asterisk* in the right column) following MP-TSCPC 180 J. Left column represents ×40, and the right column ×100.

Results

The Change in IOP

The mean IOP was changed after laser intervention and although there was no significant difference in the IOP between the groups before the laser intervention ($P = 0.117$), significant differences in the IOP were observed at 30 min and 4 weeks post-treatment between the groups ($P < 0.001$ at both time points) (Supplementary Table S1).

Structural Changes in the Uvea

Histologic examination with H&E staining confirmed the changes in the uvea, including the pars plicata and ciliary muscle, after TSCPC (Fig. 1). Following MP-TSCPC 60 J, no significant change was observed in the nonpigmented and pigmented ciliary epithelium layers in the pars plicata. Although CW-TSCPC showed atrophy of the nonpigmented and pigmented ciliary epithelium layer in a part of the pars plicata, significant destruction of the structure was not observed. However, with MP-TSCPC 120 J, 180 J, 240 J, and 300 J, partial atrophy of the pars plicata, partial disruption of nonpigmented and pigmented ciliary epithelium layers in the pars plicata, and stromal destruction in the pars plicata were observed. In addition, structural destruction of the ciliary muscle was also observed with MP-TSCPC 240 J and 300 J.

TM lengths in control, and following MP-TSCPC at 60 J, 120 J, 180 J, 240 J, and 300 J, and CW-TSCPC were estimated to be 565.61 ± 79.07 µm, 807.86 ± 75.73 µm, 733.15 ± 58.11 µm, 701.08 ± 65.73 µm, 798.22 ± 142.76 µm, 789.98 ± 120.96 µm, and 810.22 ± 128.07 µm, respectively. All TM lengths after MP-TSCPC 60 J, 120 J, 180 J, 240 J, and 300 J, and CW-TSCPC were found to increase, compared with the control ($P < 0.001$, for all) (Fig. 2). With the increase in energy of MP-TSCPC from 60 J to 180 J, the TM length decreased (MP-TSCPC 60 J vs. MP-TSCPC 120 J, $P = 0.034$; MP-TSCPC 60 J vs. MP-TSCPC 180 J, $P = 0.004$). The TM lengths after MP-TSCPC at 240 J and 300 J, and CW-TSCPC were significantly longer than those with MP-TSCPC 180 J (MP-TSCPC 180 J vs. MP-TSCPC 240 J, $P = 0.009$; MP-TSCPC 180 J vs. MP-TSCPC 300 J, $P = 0.033$; MP-TSCPC 180 J vs. CW-TSCPC, $P = 0.007$). The TM lengths after treatments with MP-TSCPC at 240 J, and 300 J were not significantly different from those with CW-TSCPC (MP-TSCPC 240 J vs. CW-TSCPC, $P = 0.865$; MP-TSCPC 300 J vs. CW-TSCPC, $P = 0.007$).

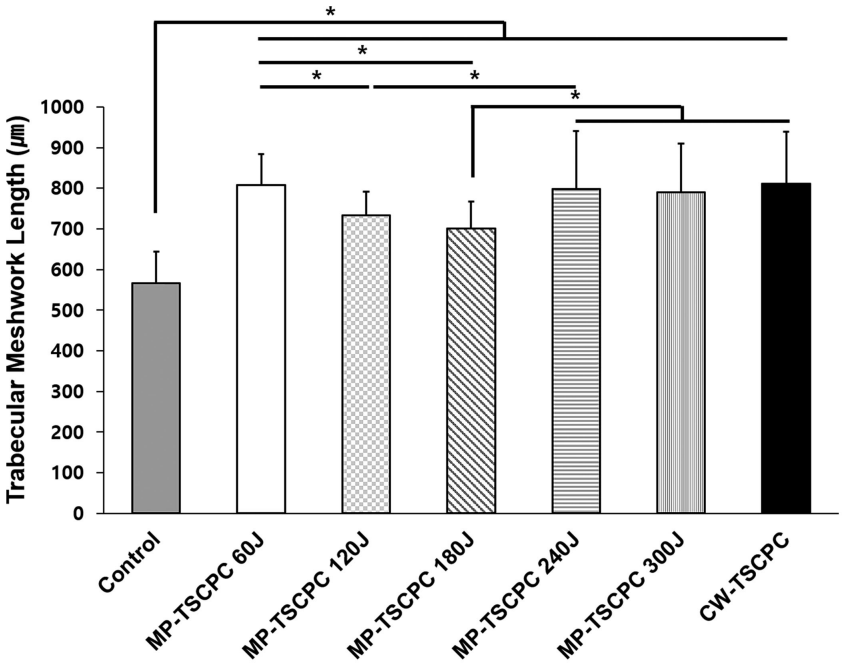

Figure 2. Comparison of TM length in control and after MP-TSCPC 60 J, MP-TSCPC 120 J, MP-TSCPC 180 J, MP-TSCPC 240 J, MP-TSCPC 300 J and CW-TSCPC. All TM lengths after MP-TSCPC 60 J, 120 J, 180 J, 240 J, and 300 J, and CW-TSCPC were higher than those of the controls. With the increase in the MP-TSCPC energy level from 60 J to 180 J, the TM length becomes shorter. TM lengths in the MP-TSCPC 240 J and 300 J, and CW-TSCPC groups are significantly longer than those in the MP-TSCPC 180 J group.

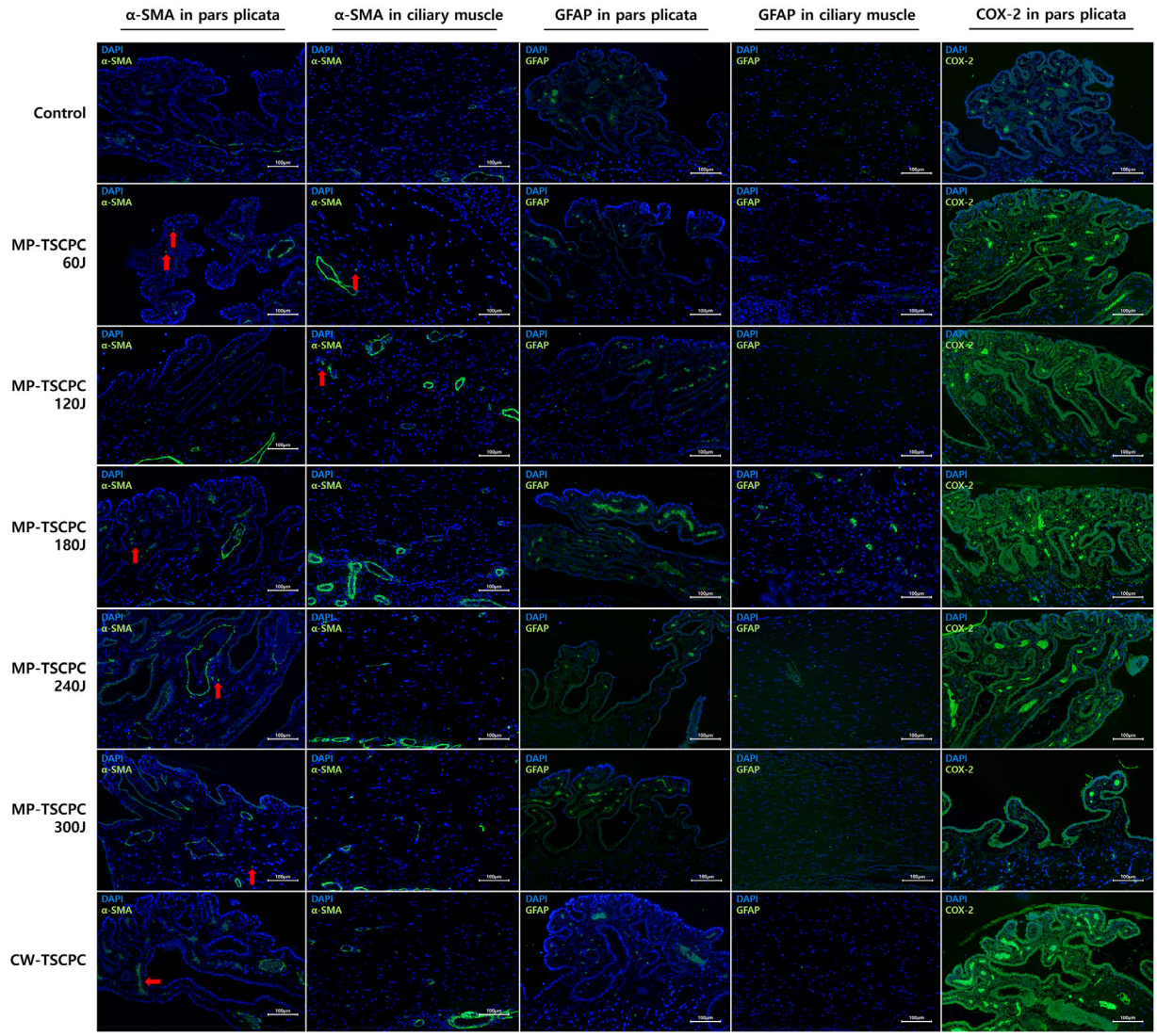

Figure 3. Immunohistochemistry with α-SMA and GFAP stainings in the pars plicata and ciliary muscle, and cyclo-oxygenase-2 (COX-2) staining in the pars plicata. The expression of α-SMA in the pars plicata and ciliary muscle was found after MP-TSCPC and CW-TSCPC (*red arrow*). GFAP expression was found in the pars plicata after MP-TSCPC and CW-TSCPC. The expression of GFAP in the ciliary muscle increased following treatment with MP-TSCPC 180 J. The expression of COX-2 was increased in the pars plicata of the MP-TSCPC and CW-TSCPC groups.

Analysis of the Expression With Immunohistochemistry Staining in the Uvea

The expression of α-SMA correlates with the activation of myofibroblasts; the expression of stromal myofibroblasts in the pars plicata was observed after MP-TSCPC and CW-TSCPC (Fig. 3). The expression areas of α-SMA in the pars plicata were measured as 841.07 ± 430.89 μm^2, 570.72 ± 419.34 μm^2, 857.42 ± 694.83 μm^2, 1429.22 ± 845.98 μm^2, 2729.53 ± 1369.63 μm^2, 1621.67 ± 1035.94 μm^2, and 1600.94 ± 1088.29 μm^2 in controls, and after MP-TSCPC at 60 J, 120 J, 180 J, 240 J, and 300 J, and CW-TSCPC respectively. The α-SMA expression increased with an increase in the energy of MP-TSCPC from 60 J to 240 J. The α-SMA expression, with high energy levels of MP-TSCPC (240 J and 300 J) or CW-TSCPC, was found to increase significantly compared with that in controls ($P = 0.045$, $P < 0.001$, and $P = 0.014$, respectively) (Fig. 4A). The expression of α-SMA also significantly differed between the MP-TSCPC groups with relatively low energy levels (60 J and 120 J) and those with high energy levels (240 J and 300 J) or CW-TSCPC (MP-TSCPC 60 J vs. MP-TSCPC 240 J, MP-TSCPC 300 J, CW-TSCPC, $P < 0.001$, $P = 0.002$, and $P = 0.001$, respectively; MP-TSCPC 120 J vs. MP-TSCPC 240 J, MP-TSCPC 300 J, CW-TSCPC, $P < 0.001$, $P = 0.02$, and $P = 0.033$, respectively) (Fig. 4A).

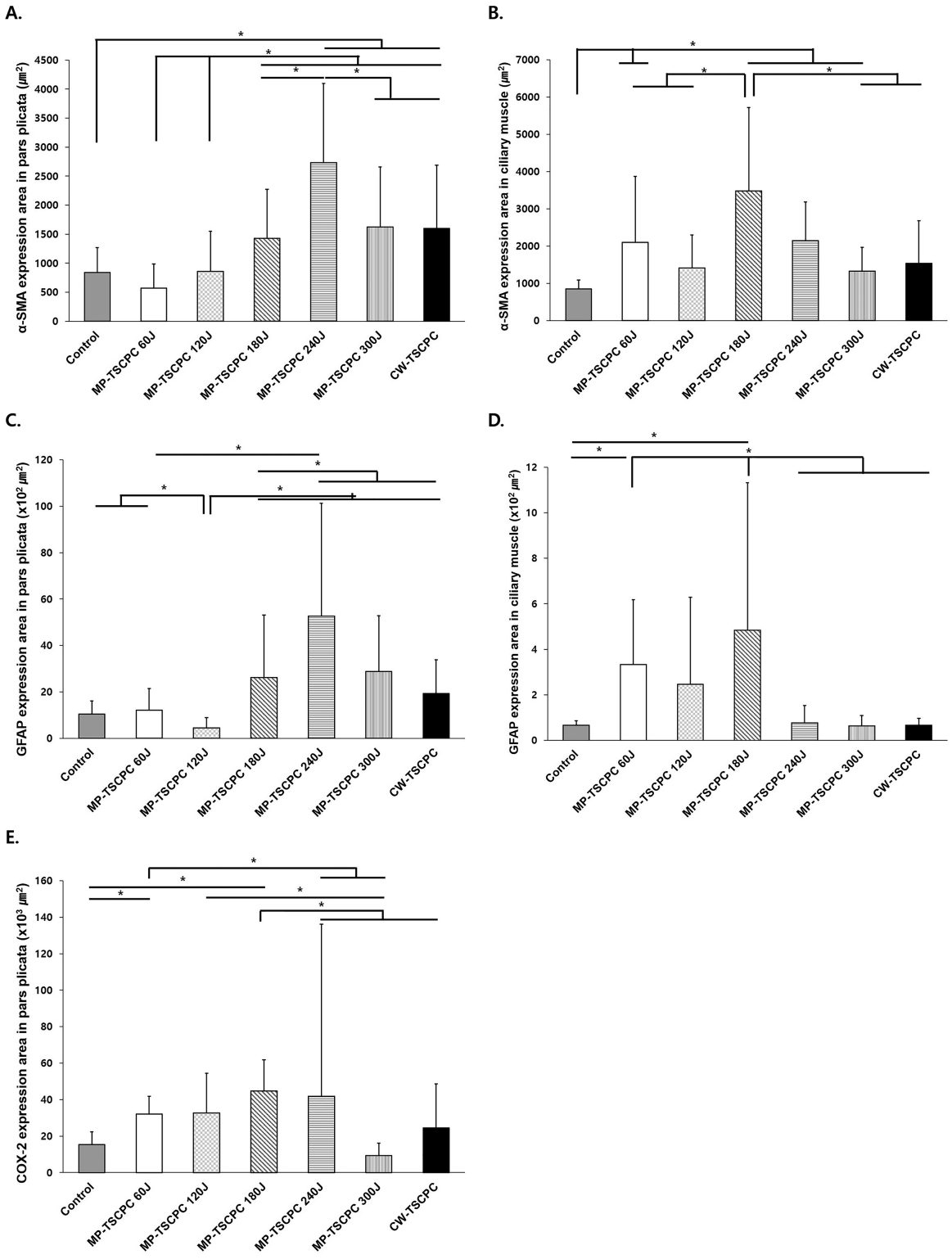

Figure 4. Expression of α-SMA staining and GFAP staining in both the pars plicata and ciliary muscle, and cyclo-oxygenase-2 (COX-2) staining in the pars plicata. With the increase in MP-TSCPC energy level from 60 J to 240 J, α-SMA expression in the pars plicata increased (A). α-SMA expression in the pars plicata significantly differed between the relatively low (60 J and 120 J) and high (240 J and 300 J) energy levels of MP-TSCPC or CW-TSCPC (A). Compared with the control group, α-SMA expression in the ciliary muscle significantly increased in all the MP-TSCPC groups, except MP-TSCPC 120 J, whereas there was no difference with CW-TSCPC (B). α-SMA expression in the MP-TSCPC 180 J group was higher than that in the other laser intervention groups (B). GFAP expression in the pars plicata relatively increased following MP-TSCPC with high energy levels (180 J, 240 J, and 300 J) and CW-TSCPC compared with MP-TSCPC with low energy levels (60 J and 120 J) (C). Compared with the control, GFAP expression in the ciliary muscle significantly increased following MP-TSCPC 60 J and 180 J (D). MP-TSCPC

→

←
60 J and 180 J induced an increase in GFAP expression compared with MP-TSCPC 240 J and 300 J, and CW-TSCPC (D). COX-2 expression in the pars plicata decreased after MP-TSCPC 240 J and 300 J, and CW-TSCPC, whereas its expression gradually increased with an increase in the energy of MP-TSCPC from 60 J to 180 J (E).

GFAP, a marker of inflammation, was expressed in the pars plicata after MP-TSCPC and CW-TSCPC (Figs. 3 and 4C). The expression areas of GFAP in the pars plicata were found to be 1641.98 ± 565.01 μm^2, 1212.90 ± 934.31 μm^2, 449.58 ± 438.31 μm^2, 2615.64 ± 2697.09 μm^2, 5270.88 ± 4858.05 μm^2, 2879.39 ± 2397.59 μm^2, and 1936.90 ± 1451.85 μm^2 in controls, and after MP-TSCPC at 60 J, 120 J, 180 J, 240 J, and 300 J, and CW-TSCPC respectively. GFAP expression did not differ between the control and after MP-TSCPC or CW-TSCPC, except MP-TSCPC 120 J (control vs. MP-TSCPC 60 J, 120 J, 180 J, 240 J, and 300 J and CW-TSCPC, $P = 0.376$, $P = 0.048$, $P = 0.921$, $P = 0.233$, $P = 0.536$, and $P = 0.959$, respectively) (Fig. 4C). However, the GFAP expression levels after high energy levels of MP-TSCPC (180 J, 240 J, and 300 J) and CW-TSCPC were relatively higher than those in MP-TSCPC (60 J and 120 J). The GFAP expression levels between MP-TSCPC 60 J and 240 J, and between MP-TSCPC 120 J and high energy levels (240 J and 300 J) or CW-TSCPC were significantly different (MP-TSCPC 60 J vs. MP-TSCPC 240 J, $P = 0.01$; MP-TSCPC 120 J vs. MP-TSCPC 180 J, 240 J, and 300 J, and CW-TSCPC, $P = 0.05$, $P < 0.001$, $P < 0.001$, and $P = 0.07$, respectively) (Fig. 4C).

COX-2 expression, a marker for staining in nonpigmented ciliary epithelium and inflammation, was relatively increased in the pars plicata after MP-TSCPC, except for MP-TSCPC 300 J and CW-TSCPC (Figs. 3 and 4E). The expression areas of COX-2 in the pars plicata were measured as 15,333.24 ± 7076.78 μm^2, 32,008.49 ± 9804.16 μm^2, 32,635.70 ± 21,883.00 μm^2, 44,666.24 ± 17,103.32 μm^2, 41,782.15 ± 94,460.90 μm^2, 9346.07 ± 6777.06 μm^2, and 24,515.41 ± 24,083.23 μm^2 in controls, and after MP-TSCPC with 60 J, 120 J, 180 J, 240 J, and 300 J, and CW-TSCPC, respectively. Although COX-2 expression was relatively decreased after treatment with MP-TSCPC 240 J and 300 J, and CW-TSCPC, a gradual increase in the expression was observed with an increase in the MP-TSCPC energy from 60 J to 180 J (Fig. 4E). MP-TSCPC 60 J and 180 J particularly induced an increase in COX-2 expression compared with the controls ($P = 0.008$ and $P < 0.001$, respectively). COX-2 expression levels after MP-TSCPT 180 J were also significantly higher than those with MP-TSCPC 240 J and 300 J, and CW-TSCPC ($P = 0.001$, $P < 0.001$, and $P = 0.024$, respectively). However, with MP-TSCPC 300 J, COX-2 expression was significantly decreased compared with MP-TSCPC 60 J, 120 J, and 180 J (MP-TSCPC 300 J vs. MP-TSCPC 60 J, $P < 0.001$; MP-TSCPC 300 J vs. 120 J, $P = 0.001$). COX-2 expression in CW-TSCPC did not differ from that in the controls or after MP-TSCPC at all energy levels, except MP-TSCPC 180 J (CW-TSCPC vs. control, MP-TSCPC 60 J, 120 J, 240 J, and 300 J, $P = 0.750$, $P = 0.247$, $P = 0.160$, $P = 0.843$, and $P = 0.160$, respectively).

Staining with α-SMA revealed that its expression in stromal myofibroblasts and smooth muscle in the vessel was increased in the ciliary muscle after MP-TSCPC and CW-TSCPC (Figs. 3 and 4B). The expression areas of α-SMA in the ciliary muscle were found to be 852.67 ± 240.49 μm^2, 2110.49 ± 1768.19 μm^2, 1408.37 ± 891.09 μm^2, 3477.39 ± 2238.54 μm^2, 2147.86 ± 1039.68 μm^2, 1327.24 ± 640.96 μm^2, and 1532.32 ± 1145.52 μm^2 in controls, and after MP-TSCPC at 60 J, 120 J, 180 J, 240 J and 300 J, and CW-TSCPC respectively. Compared with the controls, α-SMA expression levels were significantly increased at all energy levels of MP-TSCPC, except MP-TSCPC 120 J, whereas there was no difference when compared with CW-TSCPC (control vs. MP-TSCPC 60 J, 120 J, 180 J, 240 J, and 300 J, and CW-TSCPC, $P = 0.016$, $P = 0.06$, $P < 0.001$, $P = 0.01$, $P = 0.04$, and $P = 0.689$, respectively). Expression of α-SMA was found to increase with MP-TSCPC 180 J, compared with other laser interventions (MP-TSCPC 180 J vs. MP-TSCPC 60 J, 120 J, and 300 J, and CW-TSCPC, $P = 0.028$, $P = 0.001$, $P = 0.001$, and $P = 0.014$, respectively).

The expression areas of GFAP in the ciliary muscle were measured as 66.86 ± 19.50 μm^2, 334.32 ± 284.87 μm^2, 246.87 ± 381.94 μm^2, 483.54 ± 648.35 μm^2, 76.99 ± 75.54 μm^2, 76.99 ± 75.54 μm^2, and 66.91 ± 29.53 μm^2 in controls, and after MP-TSCPC at 60 J, 120 J, 180 J, 240 J, and 300 J, and CW-TSCPC. Compared with the controls, GFAP expression after MP-TSCPC 60 J and 180 J significantly increased ($P = 0.027$ and $P = 0.037$, respectively). MP-TSCPC 60 J and 180 J also induced an increase in GFAP expression compared with MP-TSCPC 240 J and 300 J, and CW-TSCPC (MP-TSCPC 60 J vs. MP-TSCPC 240 J, and 300 J, and CW-TSCPC, $P = 0.001$, $P = 0.001$, and $P = 0.002$, respectively; MP-TSCPC 180 J vs. MP-TSCPC 240 J, and 300 J, and CW-TSCPC, $P = 0.004$, $P = 0.001$, and $P = 0.008$, respectively) (Figs. 3 and 4D).

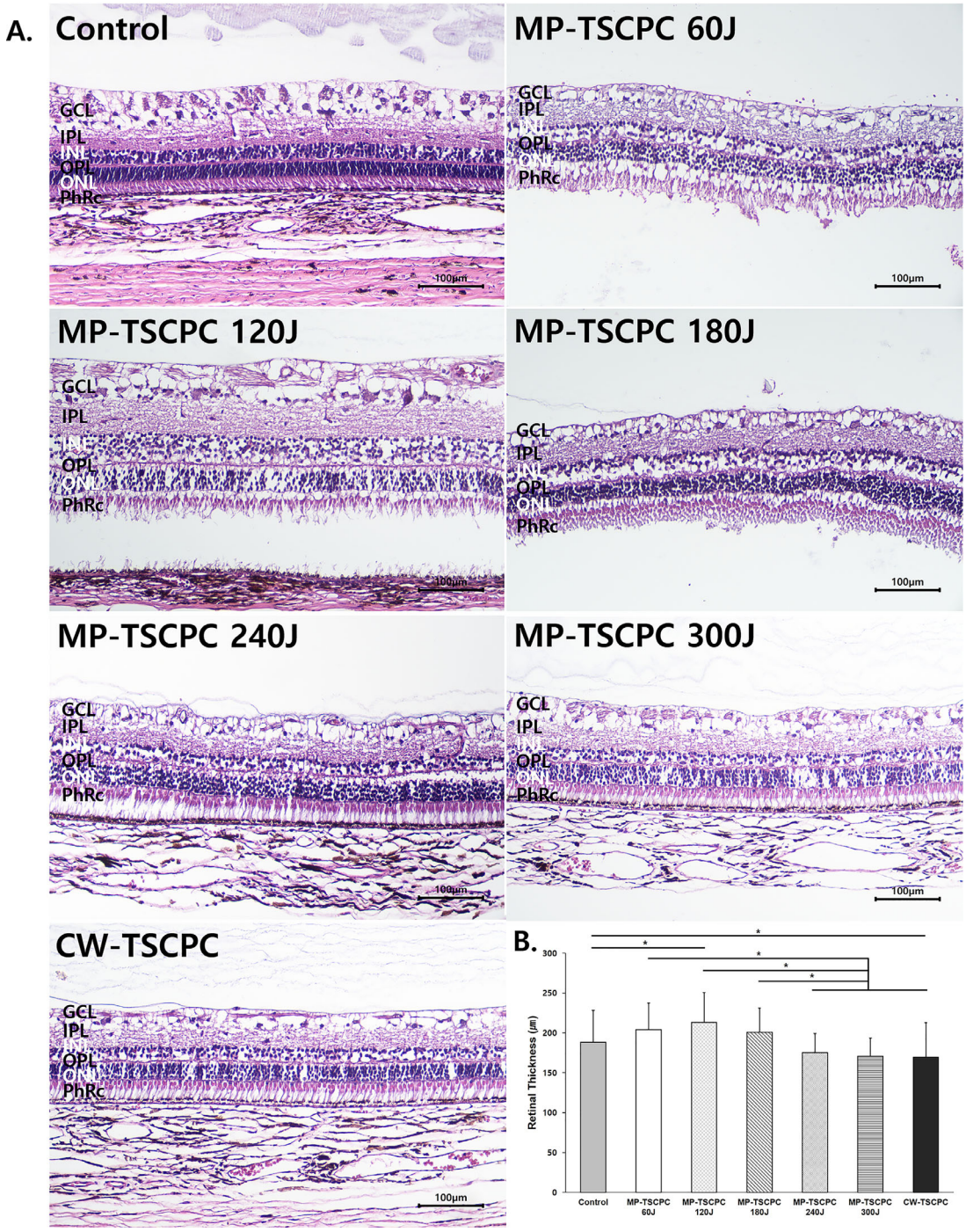

Figure 5. Histologic examination using H&E staining (A) and retinal thickness in controls and after MP-TSCPC or CW-TSCPC (B). All layers of the retina, including the ganglion cell layer (GCL), inner plexiform layer (IPL), inner nuclear layer (INL), outer plexiform layer (OPL), and photoreceptor layer (PhRc), showed relatively intact morphology with either MP-TSCPC or CW-TSCPC (A). There was no disruption of the retinal layers after MP-TSCPC and CW-TSCPC (A). Compared with the controls, retinal thickness slightly increased with MP-TSCPC 120 J but decreased with CW-TSCPC (B). In particular, retinal thicknesses with MP-TSCPC 240 J and 300 J and CW-TSCPC were significantly lower than those with MP-TSCPC 60 J, 120 J, and 180 J (B).

Structural Changes and the Analysis of the Expression After Immunohistochemistry Staining of the Retina

Histologic examination using H&E staining was used to analyze the structural changes in the retina. All layers of the retina, including the ganglion cell layer, inner plexiform layer, inner nuclear layer, outer plexiform layer, and photoreceptor layer, showed relatively intact morphologies, indicating no disruption, despite treatment with MP-TSCPC or CW-TSCPC (Fig. 5A). The retinal thicknesses of whole retinal layers were found to be 188.29 ± 39.87 μm, 204.03 ± 33.51 μm, 213.32 ± 37.24 μm, 200.74 ± 30.56 μm, 175.08 ± 24.28 μm, 170.73 ± 22.88 μm, and 169.80 ± 42.96 μm in controls, and after MP-TSCPC at 60 J, 120 J, 180 J, 240 J, and 300 J and CW-TSCPC, respectively. Compared with the controls, the retinal thickness increased slightly after MP-TSCPC 120 J intervention ($P = 0.013$) and decreased after CW-TSCPC ($P = 0.044$) (Fig. 5B). In particular, the retinal thickness following MP-TSCPC 240 J, and 300 J, and CW-TSCPC significantly decreased compared with that after MP-TSCPC 60 J, 120 J, and 180 J (MP-TSCPC 240 J vs. 60 J, 120 J, 180 J, $P < 0.001$, $P = 0.001$, and $P = 0.005$, respectively; MP-TSCPC 300 J vs. 60 J, 120 J, 180 J, $P < 0.001$, $P < 0.001$, and $P = 0.001$, respectively; CW-TSCPC vs. 60 J, 120 J, 180 J, $P = 0.002$, $P = 0.001$, and $P < 0.001$, respectively). Although the morphology of each retinal layer was not disrupted, the retinal thickness could change when atrophy occurred in some retinas, under the influence of a laser.

Immunohistochemistry was performed, with GFAP staining in the retina, and the expression of GFAP in the control was observed only in the ganglion cell layer, where glial cells were normally distributed (Fig. 6A). However, GFAP expression was observed in other layers following MP-TSCPC or CW-TSCPC. In the quantitative analysis of GFAP expression in the retina, there was no difference among the control, MP-TSCPC, and CW-TSCPC groups ($P = 0.826$) (Fig. 6B). The mean areas of GFAP expression were 15,377.67 ± 3144.51 μm^2, 12,803.58 ± 2557.68 μm^2, 15,581.71 ± 6623.35 μm^2, 13,860.43 ± 4421.69 μm^2, 13,539.84 ± 3356.49 μm^2, 13944.61 ± 3226.96 μm^2, and 14,313.06 ± 3904.19 μm^2 in controls, and after MP-TSCPC at 60 J, 120 J, 180 J, 240 J, and 300 J, and CW-TSCPC, respectively.

Discussion

In this study, the effects of different energy levels of MP-TSCPC, compared with those of CW-TSCPC, were analyzed for the uvea and retina. MP-TSCPC 60 J and 120 J affected the ciliary muscle more than they affected the pars plicata, and MP-TSCPC of more than 180 J induced histologic changes in both the pars plicata and ciliary muscle. Histology and immunohistochemistry revealed minimal changes in the retina, although retinal thickness was found to increase after MP-TSCPC 120 J.

In a previous study, low, moderate, and high energy levels of MP-TSCPC were defined as less than 100 J, 112 to 140 J, and approximately 200 J, respectively.[3] Based on the energy levels, the effects and complications of MP-TSCPC could vary. Low energy levels did not invoke any complications, but could not successfully lower the IOP after treatment, unlike high energy levels where successful lowering of IOP was accompanied by severe complications.[6,17] However, there has been no report describing a direct comparison of the changes in the uvea and retina with an increase in the energy levels of MP-TSCPC. In this study, we performed MP-TSCPC treatment at different total energy levels. Based on previous studies,[3,6,17] MP-TSCPC at 60 J can be classified as low energy level, 120 J as moderate energy level, 180 J as moderate-to-high energy level, and 240 J and 300 J as high energy levels. During the experiment, a pop sound, which indicates overtreatment of ciliary body, was heard one to two times at 300 J. Unlike CW-TSCPC, a pop sound was not occurred while performing MP-TSCPC because the laser probe was applied to the scleral area in a continuous sliding arc motion rather than in a specific location. Therefore, there was no pop sound from 60 J to 240 J, but a pop sound occurred at 300 J as the accumulated energy level increased.

Although the mechanism of action of MP-TSCPC is not yet clear, there are some hypotheses regarding it.[3] The results of this study support this hypothesis. First, although CW-TSCPC directly destroys the ciliary epithelium in the pars plicata through thermal stimulation, the ciliary epithelium is not necessarily involved in the mechanism of action after MP-TSPC.[3,18] It acts on the ciliary muscle rather than the pars plicata without destroying tissues. Therefore, because of this characteristic, some researchers have suggested that it is called micropulse transscleral laser therapy rather than MP-TSCPC.[5,19] In this study, immunohistochemistry with α-SMA and GFAP staining revealed the occurrence of inflammation in the ciliary muscle, whereas histologic examinations did not indicate any change in the pars plicata after MP-TSCPC at a low energy level. However, CW-TSCPC and MP-TSCPC at high energy levels induced the occurrence of inflammation and histologic changes in both the ciliary muscle and pars plicata. It is speculated that high energy levels

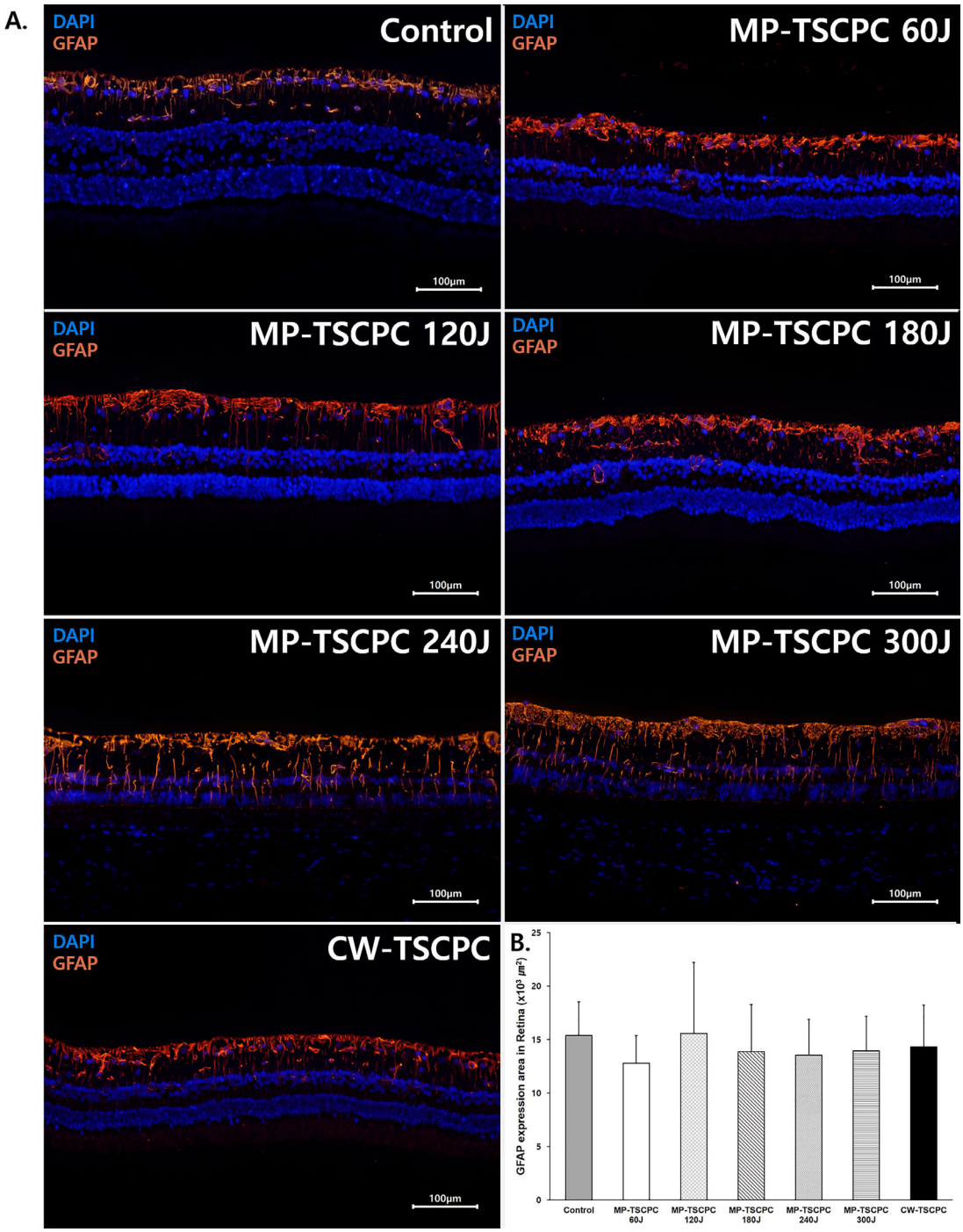

Figure 6. Immunohistochemistry with GFAP staining in the retina (A) and quantitative analysis of GFAP expression in retina among the control, MP-TSCPC, and CW-TSCPC groups (B). GFAP staining revealed that the expression of GFAP in the control was located in the ganglion cell layer, where glial cells were normally distributed (A). GFAP expression was observed in other layers after MP-TSCPC or CW-TSCPC. Quantitative analysis of GFAP expression in the retina showed no difference among the control, MP-TSCPC, and CW-TSCPC groups (B).

induce damage by transferring heat to the adjacent pars plicata.[3,20] MP-TSCPC at low to moderate energy levels acts on the ciliary muscle rather than the pars plicata. Second, MP-TSCPC is known to act on the ciliary muscle and induce displacement of the sclera spur in a posterior and inward direction.[3] The length of the TM is changed according to the location of the scleral spur.[15,16] The scleral spur is located at

the junction of the ciliary muscle[15]; therefore, if the ciliary muscle is affected, the locations of the scleral spur and TM length can change.[21] In this study, we found a change in the TM length after MP-TSCPC. Immunohistochemistry revealed that the lower energy level of MP-TSCPC acts on the ciliary muscle rather than the pars plicata and the moderate energy level of MP-TSCPC acts on both the ciliary muscle and pars plicata. Therefore, TM length increased the most after MP-TSCPC 60 J, and TM length was decreased the most after MP-TSCPC 180 J. Because the ciliary muscle was destroyed after the high energy level of MP-TSCPC, it could be measured with a long length. Our results provide evidence to support the hypothesis for the mechanism of action of MP-TSCPC, which can affect the ciliary muscle and change the TM outflow by changing the position of the scleral spur.

The retina is far from the ciliary muscle and pars plicata, where the TSCPC is applied. However, some reports have indicated that MP-TSCPC can affect the choroidal thickness and lead to cystoid macular edema.[7,22] Although immunohistochemistry with GFAP staining did not reveal any significant difference in the retina after 1 month after TSCPC treatment, GFAP staining showed a slight increase in inflammation induced by MP-TSCPC 120 J, thereby leading to an increase in retinal thickness. In contrast, the retinal thickness upon treatment with MP-TSCPC at high energy levels and CW-TSCPC was lower than that observed after MP-TSCPC at other energy levels. Because TSCPC can cause thermal transfer from the sclera to the retina, its effect might be greater with higher energy levels, which leads to retinal thinning.[23,24] Therefore, our histologic studies revealed that MP-TSCPC directly affects the uvea, but indirectly affects the retina.

This study had some limitations. First, a relatively small number of animals were included in each group. Because we sought to compare several energy levels of MP-TSCPC and to observe the change at 1 month beyond the treatment, rather than an acute change immediately after the laser treatment, the number of animals per groups was limited to minimize the number of animals sacrificed. Second, histologic changes may not be evident in some tissues. CW-TSCPC was applied only on 20 sites of a total of 360° with a safety energy level because of the laser protocol to avoid severe complications. Usually, when setting the power of the CW-TSCPC in the clinic, the power is increased until a pop sound is heard.[2] We set the lower level of power for safety, and our energy level was also sufficient to seem to be effective according to a previous report.[5] Although MP-TSCPC was performed at almost 360° except at the 3 and 9 o'clock positions, a uniform change may not occur. In addition, because the probes of MP-TSCPC and CW-TSCPC were different, the location where the laser was performed might not be exactly the same. To minimize this limitation in this study, the tissues were sectioned in at least four places per eye, including the pars plicata and ciliary muscle, and the experiments were conducted on three eyes per group. Third, there were some differences of ocular anatomy between pigs and humans. The axial length in pigs is shorter than that in humans, which could have affected the results. The mean axial length in human adults is approximately 22 to 25 mm. The axial length in pigs was measured to be approximately 20 mm in this study. However, MP-TSCPC has also been performed in pediatric patients and other animals. The axial length in pediatric patients is shorter than that in human adults, and pediatric patients showed similar effects of laser treatment to those of adults.[25] Besides, some researchers reported the good effect of MP-TSCPC in dogs.[10,26,27] Dogs have an axial length approximately 21 mm shorter than human adults.[14] The size of ciliary muscle in porcine eyes was smaller than humans.[28] Considering that the length of the ciliary body also varies according to the axial length in humans and MP-TSCPC could be applied to pediatric patients, there would be minimal difference in effectiveness when performing MP-TSCPC in porcine eyes when compared to humans.[25,29] The ciliary body of porcine eyes was located posterior to the iris and anterior to the retina, the same as in humans. Because the size and anatomy of the porcine eye and the human eye are relatively similar, porcine eyes have been widely used in experiments.[30] In contrast, the degree of pigmentation in the ciliary body was greater in porcine eyes than in human eyes,[28] and the energy levels for a similar effect of laser treatment in pigs could be lower than those in humans.[31,32] Fourth, the purpose of this study was to determine any chronic effects of MP-TSCPC by observing the inflammatory state and histologic changes 1 month after the treatment, and not the immediate changes after the laser treatment. In particular, because the retina is not directly irradiated, the change is relatively small at 1 month after the laser treatment.

In conclusion, the histologic changes in the uvea and peripheral retina after laser intervention were different according to the types of laser application and levels of energy. MP-TSCPC with lower energy levels mainly affected the ciliary muscle without changes in the peripheral retina or the pars plicata. However, MP-TSCPC with high energy levels affected both the ciliary

muscle and pars plicata. Our results may imply the possibility of intraocular damage in humans according to the different levels of energy.

Acknowledgments

Supported in part by the Bio & Medical Technology Development Program of the NRF funded in part by the Korean government and the Ministry of Science and ICT (MSIP) (NRF- 2017M3A9E2056458, and 2020R1A2C1005729). This research was also supported by a Korea University Guro Hospital Grant (O1905421). The sponsor or funding or organization had no role in the design or conduct of this research.

Author contributions: Study design (S.M.A., S.K.); study conduct (S.M.A., M.C., S.K.); data collection (S.M.A.); data analysis and interpretation (S.M.A., S.K., Y.Y.K.); and preparation, review, and approval of the manuscript (S.M.A., M.C., S.K., Y.Y.K.).

Disclosure: **S.M. Ahn,** None; **M. Choi,** None; **S.-W. Kim,** None; **Y.Y. Kim,** None

References

1. Scholz P, Altay L, Fauser S. A review of subthreshold micropulse laser for treatment of macular disorders. *Adv Ther*. 2017;34:1528–1555.
2. Dastiridou AI, Katsanos A, Denis P, et al. Cyclodestructive procedures in glaucoma: a review of current and emerging options. *Adv Ther*. 2018;35:2103–2127.
3. Sanchez FG, Peirano-Bonomi JC, Grippo TM. Micropulse transscleral cyclophotocoagulation: a hypothesis for the ideal parameters. *Med Hypothesis Discov Innov Ophthalmol*. 2018;7:94–100.
4. Aquino MC, Barton K, Tan AM, et al. Micropulse versus continuous wave transscleral diode cyclophotocoagulation in refractory glaucoma: a randomized exploratory study. *Clin Exp Ophthalmol*. 2015;43:40–46.
5. Souissi S, Le Mer Y, Metge F, et al. An update on continuous-wave cyclophotocoagulation (CW-CPC) and micropulse transscleral laser treatment (MP-TLT) for adult and paediatric refractory glaucoma. *Acta Ophthalmol*. 2020;99:e621–e3653.
6. Williams AL, Moster MR, Rahmatnejad K, et al. Clinical efficacy and safety profile of micropulse transscleral cyclophotocoagulation in refractory glaucoma. *J Glaucoma*. 2018;27:445–449.
7. Barac R, Vuzitas M, Balta F. Choroidal thickness increase after micropulse transscleral cyclophotocoagulation. *Rom J Ophthalmol*. 2018;62:144–148.
8. Hennis HL, Stewart WC. Semiconductor diode laser transscleral cyclophotocoagulation in patients with glaucoma. *Am J Ophthalmol*. 1992;113:81–85.
9. Ishida K. Update on results and complications of cyclophotocoagulation. *Curr Opin Ophthalmol*. 2013;24:102–110.
10. Sebbag L, Allbaugh RA, Strauss RA, et al. MicroPulse transscleral cyclophotocoagulation in the treatment of canine glaucoma: preliminary results (12 dogs). *Vet Ophthalmol*. 2019;22:407–414.
11. Tan AM, Chockalingam M, Aquino MC, Lim ZI, See JL, Chew PT. Micropulse transscleral diode laser cyclophotocoagulation in the treatment of refractory glaucoma. *Clin Exp Ophthalmol*. 2010;38:266–272.
12. Zaarour K, Abdelmassih Y, Arej N, Cherfan G, Tomey KF, Khoueir Z. Outcomes of micropulse transscleral cyclophotocoagulation in uncontrolled glaucoma patients. *J Glaucoma*. 2019;28:270–275.
13. Ahn SM, Ahn J, Cha S, et al. Development of a post-vitrectomy injection of N-methyl-N-nitrosourea as a localized retinal degeneration rabbit model. *Exp Neurobiol*. 2019;28:62–73.
14. Ahn SM, Ahn J, Cha S, et al. Morphologic and electrophysiologic findings of retinal degeneration after intravitreal sodium iodate injection following vitrectomy in canines. *Sci Rep*. 2020;10:3588.
15. Choi W, Lee MW, Kang HG, et al. Comparison of the trabecular meshwork length between open and closed angle with evaluation of the scleral spur location. *Sci Rep*. 2019;9:6857.
16. Kasuga T, Chen YC, Bloomer MM, et al. Trabecular meshwork length in men and women by histological assessment. *Curr Eye Res*. 2013;38:75–79.
17. Sanchez FG, Lerner F, Sampaolesi J, et al. Efficacy and safety of Micropulse(R) transscleral cyclophotocoagulation in glaucoma. *Arch Soc Esp Oftalmol*. 2018;93:573–579.
18. Johnstone M, Wang R, Padilla S, Wen K. Transcleral laser induces aqueous outflow pathway motion and reorganization (abstract). 27th Annual Meeting of the American Glaucoma Society Annual Meeting. 2017.
19. Magacho L, Lima FE, Avila MP. Double-session micropulse transscleral laser (CYCLO G6) as a

primary surgical procedure for glaucoma. *J Glaucoma*. 2020;29:205–210.
20. Pantcheva MB, Kahook MY, Schuman JS, Noecker RJ. Comparison of acute structural and histopathological changes in human autopsy eyes after endoscopic cyclophotocoagulation and trans-scleral cyclophotocoagulation. *Br J Ophthalmol*. 2007;91:248–252.
21. Moses RA, Grodzki WJ, Jr. The scleral spur and scleral roll. *Invest Ophthalmol Vis Sci*. 1977;16:925–931.
22. Yelenskiy A, Gillette TB, Arosemena A, et al. Patient outcomes following micropulse transscleral cyclophotocoagulation: intermediate-term results. *J Glaucoma*. 2018;27:920–925.
23. Regal S, O'Connor D, Brige P, Delattre R, Djenizian T, Ramuz M. Determination of optical parameters of the porcine eye and development of a simulated model. *J Biophotonics*. 2019;12:e201800398.
24. Regal S, Troughton J, Delattre R, Djenizian T, Ramuz M. Changes in temperature inside an optomechanical model of the human eye during emulated transscleral cyclophotocoagulation. *Biomed Opt Express*. 2020;11:4548–4559.
25. Abdelrahman AM, El Sayed YM. Micropulse versus continuous wave transscleral cyclophotocoagulation in refractory pediatric glaucoma. *J Glaucoma*. 2018;27:900–905.
26. Sapienza JS, Kim K, Rodriguez E, DiGirolamo N. Preliminary findings in 30 dogs treated with micropulse transscleral cyclophotocoagulation for refractory glaucoma. *Vet Ophthalmol*. 2019;22:520–528.
27. Story BD, Sapienza JS, Di Girolamo N, Kim K. Long-term results (>1 year) in 19 dogs treated with MicroPulse transscleral diode cyclophotocoagulation for refractory glaucoma. *Vet Ophthalmol*. 2021 May 26 [Epub ahead of print].
28. Sanchez I, Martin R, Ussa F, Fernandez-Bueno I. The parameters of the porcine eyeball. *Graefes Arch Clin Exp Ophthalmol*. 2011;249:475–482.
29. Okamoto Y, Okamoto F, Nakano S, Oshika T. Morphometric assessment of normal human ciliary body using ultrasound biomicroscopy. *Graefes Arch Clin Exp Ophthalmol*. 2017;255:2437–2442.
30. May CA, Skorski LM, Lutjen-Drecoll E. Innervation of the porcine ciliary muscle and outflow region. *J Anat*. 2005;206:231–236.
31. Edmiston AM, SooHoo JR, Seibold LK, Kahook MY, Palestine AG, Pantcheva MB. Postoperative inflammation after endoscopic cyclophotocoagulation: racial distribution and effect on outcomes. *J Glaucoma*. 2018;27:266–268.
32. Pantcheva MB, Kahook MY, Schuman JS, Rubin MW, Noecker RJ. Comparison of acute structural and histopathological changes of the porcine ciliary processes after endoscopic cyclophotocoagulation and transscleral cyclophotocoagulation. *Clin Exp Ophthalmol*. 2007;35:270–274.